

# Ligand binding and antigenic properties of a human neonatal Fc receptor with mutation of two unpaired cysteine residues

Jan T. Andersen<sup>1</sup>, Sune Justesen<sup>2</sup>, Burkhard Fleckenstein<sup>3</sup>, Terje E. Michaelsen<sup>4,5</sup>, Gøril Berntzen<sup>1</sup>, Vania E. Kenanova<sup>6</sup>, Muluneh B. Daba<sup>1</sup>, Vigdis Lauvrak<sup>1,\*</sup>, Søren Buus<sup>2</sup> and Inger Sandlie<sup>1</sup>

1 Department of Molecular Biosciences and Centre for Immune Regulation, University of Oslo, Norway

2 Institute of Medical Microbiology and Immunology, University of Copenhagen, Denmark

3 Institute of Immunology and Centre for Immune Regulation, University of Oslo, Rikshospitalet University Hospital, Norway

4 Norwegian Institute of Public Health, Oslo, Norway

5 Institute of Pharmacy, University of Oslo, Norway

6 Crump Institute for Molecular Imaging, Department of Molecular and Medical Pharmacology, David Geffen School of Medicine at University of California Los Angeles, USA

## Keywords:

antigenic properties; bacterial expression; MALDI-TOF peptide mapping; soluble human neonatal Fc receptor (shFcRn); unpaired cysteines

## Correspondence

J. T. Andersen, Department of Molecular Biosciences, University of Oslo, PO Box 1041, 0316 Oslo, Norway  
Fax: +47 22 85 40 61  
Tel: +47 22 85 47 93  
E-mail: janta@imbv.uio.no, inger.sandlie@imbv.uio.no

## \*Present address

Norwegian Knowledge Centre for the Health Services, Oslo, Norway

(Received 11 April 2008, revised 6 June 2008, accepted 13 June 2008)

doi:10.1111/j.1742-4658.2008.06551.x

The neonatal Fc receptor (FcRn) is a major histocompatibility complex class I-related molecule that regulates the half-life of IgG and albumin. In addition, FcRn directs the transport of IgG across both mucosal epithelium and placenta and also enhances phagocytosis in neutrophils. This new knowledge gives incentives for the design of IgG and albumin-based diagnostics and therapeutics. To study FcRn *in vitro* and to select and characterize FcRn binders, large quantities of soluble human FcRn are needed. In this report, we explored the impact of two free cysteine residues (C48 and C251) of the FcRn heavy chain on the overall structure and function of soluble human FcRn and described an improved bacterial production strategy based on removal of these residues, yielding  $\sim 70 \text{ mg}\cdot\text{L}^{-1}$  of fermentation of refolded soluble human FcRn. The structural and functional integrity was proved by CD, surface plasmon resonance and MALDI-TOF peptide mapping analyses. The strategy may generally be translated to the large-scale production of other major histocompatibility complex class I-related molecules with nonfunctional unpaired cysteine residues. Furthermore, the anti-FcRn response in goats immunized with the FcRn heavy chain alone was analyzed following affinity purification on heavy chain-coupled Sepharose. Importantly, purified antibodies blocked the binding of both ligands to soluble human FcRn and were thus directed to both binding sites. This implies that the FcRn heavy chain, without prior assembly with human  $\beta 2$ -microglobulin, contains the relevant epitopes found in soluble human FcRn, and is therefore sufficient to obtain binders to either ligand-binding site. This finding will greatly facilitate the selection and characterization of such binders.

## Abbreviations

FcRn, the neonatal Fc receptor; GST, glutathione-S-transferase; HAT-tag, hexa-histidine tag; HC, heavy chain; HEK, human embryonic kidney; hIgG, human IgG; HSA, human serum albumin; h $\beta 2$ m, human  $\beta 2$ -microglobulin; MHC, major histocompatibility complex; RU, resonance units; SEC, size exclusion chromatography; shFcRn, soluble human FcRn; SM, skimmed milk; SPR, surface plasmon resonance;  $\beta 2$ m,  $\beta 2$ -microglobulin.

The neonatal Fc receptor (FcRn), which plays a central role in prolonging the half-life of IgG and albumin [1–3], is a major histocompatibility complex (MHC) class I-related receptor consisting of a heavy chain (HC) with three ectodomains ( $\alpha 1$ ,  $\alpha 2$  and  $\alpha 3$ ), a transmembrane part and a short intracellular signaling tail. Like MHC class I HC, the FcRn counterpart is noncovalently associated with  $\beta 2$ -microglobulin ( $\beta 2m$ ) [4,5]. Furthermore, FcRn directs the transepithelial transcytosis of maternal IgG over the intestine of neonatal rats [6,7] and is essential for human IgG transplacental transport in *ex vivo* experiments [8–10], an observation that strongly suggests a role for FcRn in the transfer of maternal IgG from mother to fetus. Moreover, FcRn-mediated transport across cellular barriers has been shown in *in vitro* intestinal cell lines, in mice and primate studies *in vivo* [11–13], and has been explored as a drug delivery pathway [11,14]. Expression of FcRn has recently been demonstrated on immune cells such as macrophages, monocytes, dendritic cells and bone marrow-derived phagocytic cells [15,16], but a complete understanding of its role in these cells is lacking, except for a report that FcRn participates in phagocytosis in neutrophils [17].

Interaction studies and crystallographic mapping have uncovered the interaction sites on both IgG and FcRn, as reviewed previously [2]. The interaction is highly pH dependent, with binding at acidic pH (pH 6.0–6.5) and no binding/release from the receptor at physiological pH (pH 7.2–7.4). A key feature is conserved histidine residues localized to the C<sub>H2</sub>–C<sub>H3</sub> interface of the IgG Fc, especially H310 and H435 that become protonated at acidic pH to interact with negatively charged residues on the  $\alpha 2$  domain of the FcRn HC [2,4,18]. Albumin also interacts, in a pH-dependent manner, with an  $\alpha 2$  domain site distally from the IgG interaction site [19], and both ligands may interact with FcRn simultaneously. Importantly, the pH dependence seems to be of fundamental importance in all FcRn-mediated functions.

The molecular understanding of the diverse functions involving FcRn is increasingly being translated into the novel design of antibody-based and albumin-based diagnostics and therapeutics, as demonstrated through the development of IgGs with increased half-life [20–22] and improved imaging properties [23–25], as well as of Fc and albumin fusion products with an increased half-life [26–29]. Furthermore, IgGs with increased binding to FcRn at physiological pH accelerate the turnover of circulating autoimmune or otherwise pathogenic IgG molecules as they block the IgG site [2,30]. Thus, development of new specific FcRn binding molecules is attractive, and approaches for

the *in vitro* selection of binders will consistently need large quantities of soluble human FcRn (shFcRn) as well as panning and elution strategies where the pH dependence of the interaction may be carefully controlled.

Four conserved cysteine residues form two disulfide bridges in the MHC class I HC. The hFcRn counterpart has, in addition, two unpaired cysteine residues [4,5] that complicate heterologous production. We have previously described successful heterologous production of truncated MHC class I molecules [31,32] and of a shFcRn wild-type (WT) receptor with native binding characteristics [33]. Here, we report on the mutation of two unpaired cysteines to serines (C48S and C251S) and expression of the double mutant HC in *Escherichia coli* followed by extraction in 8 M urea and subsequent *in vitro* refolding in the presence of human  $\beta 2$ -microglobulin (h $\beta 2m$ ). This resulted in a 10-fold increased yield. Furthermore, the structural elements were correctly formed, and stringent reversible pH-dependent binding to human IgG1 (hIgG1) as well as to human serum albumin (HSA) was demonstrated by surface plasmon resonance (SPR) measurements. Subsequently, immunization of goats with either shFcRn or the easily obtained HC gave rise to specific antibodies that inhibited the binding of both ligands – hIgG1 and albumin – to shFcRn. The HC could be covalently coupled to Sepharose to form a matrix for the purification or selection of such binders.

## Results

### Site-directed mutagenesis, expression and purification of a eukaryotic shFcRn C48S/C251S mutant

Six cysteine residues exist within the extracellular part of hFcRn HC [5], forming one disulfide bond within the  $\alpha 2$  domain (C96–C159) and one within the  $\alpha 3$  domain (C198–C252). In addition, there are two unpaired cysteine residues, namely C48 and C251, located in the  $\alpha 1$  and  $\alpha 3$  domains, respectively. The HC-associated h $\beta 2m$  has one disulfide bond (C25–C80). Figure 1A shows a crystallographic illustration of truncated shFcRn (amino acids 1–267 of HC) with the cysteine residues indicated.

To investigate the functional impact of the free cysteines, C48 and C251 were mutated to serines in the truncated HC. Both WT and mutant were expressed as glutathione-S-transferase (GST) fusions in human cells, as previously described [34]. The mutant was secreted at slightly higher levels than the WT. Both were purified and tested for functional pH-dependent

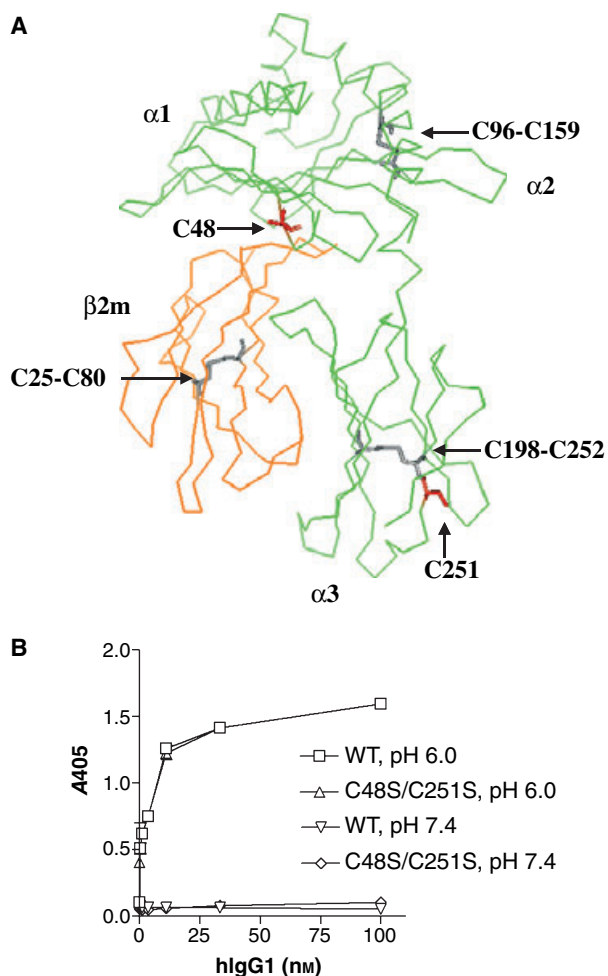


**Fig. 1.** Structure of shFcRn and pH-dependent binding of shFcRn–GST variants to hIgG1. (A) Crystallographic representation of shFcRn with the cysteine residues shown. The disulfide bonds are shown in grey and C48 as well as C251 are shown in red. The figure was designed with PYMOL using the data for shFcRn [5]. (B) Purified shFcRn WT–GST and shFcRn C48S/C251S–GST produced in 293E cells were tested for functional pH-dependent binding by ELISA. The ELISA values represent the mean of triplicates.

binding to hIgG in two different assays. First, the pH-dependent hIgG1-binding capacity of shFcRn WT–GST was compared with that of shFcRn C48S/C251S–GST. The mutant bound as strongly as the WT receptor at pH 6.0, but only weak binding of either was detected at pH 7.4 (Fig. 1B). A binding experiment using hIgG coupled to Sepharose followed by immunoblotting showed concentration-dependent binding of both shFcRn WT–GST and shFcRn C48S/C251S–GST at pH 6.0. No binding of either was observed at pH 7.4 or using uncoupled Sepharose at pH 6.0. Mutant shFcRn and WT bound IgG in the same manner (supplementary Fig. S1).

### Prokaryotic expression of hFcRn C48S/C251S HCs

To investigate the impact of C48 and C251 on heterologous production, C48S/C251S HC was produced in *E. coli* (supplementary Fig. S2) and purified as described in the Materials and methods. The yield was ~2.5-fold higher (550 mg from a 2 L fermentation) than that obtained for WT. Mutant HC was then added to an *in vitro* refolding solution together with an independently expressed and purified h $\beta$ 2m [31]. The elution profile from size-exclusion chromatography (SEC) separation of the refolded shFcRn mutant showed three peaks (EL1, EL2 and EL3; Fig. 2A). EL2 was identified as heterodimeric shFcRn, EL1 as aggregated mutant HC and EL3 as aggregated residual h $\beta$ 2m on nonreducing SDS-PAGE (Fig. 2B). The total yield of the heterodimeric shFcRn mutant was 140 mg from a 2 L fermentation, increasing the output by approximately 10-fold compared with the WT [33]. Importantly, while only 5% of the WT HCs were refolded upon exposure to h $\beta$ 2m [33], 26% of the mutant HC was incorporated in complete molecules under the same experimental conditions. Comparing this strategy with classical reduction/oxidation refolding, the latter produced large amounts of high-molecular-mass aggregates, whereas the disulfide-assisted refolding did not (supplementary Fig. S3). Comparison of expression and refolding between the WT and the mutant is summarized in the supplementary (Table S2).

### Structural and thermal stability analyses of bacterially produced shFcRn

Structural features in addition to thermal stability were determined by CD analyses. Figure 3 shows the CD spectrum for the shFcRn C48S/C251S with a typical negative peak at 217–218 nm and a positive peak at 195–197 nm. Furthermore, calculation of the secondary structural elements (Table 1) was in agreement with previously reported bacterially expressed shFcRn WT and with data obtained by others [4,5,35,36]. In addition, the thermal stability of the shFcRn mutant was demonstrated to generate a midpoint unfolding temperature of 58 °C (data not shown), similar to that of WT (58.5 °C) [33].

### Mapping of disulfide bonds by MALDI-TOF MS

To investigate the folding of the recombinant receptor variants in greater detail, disulfide mapping was performed by MALDI-TOF MS. Gel-separated protein subunits were digested by trypsin, either after alkylation

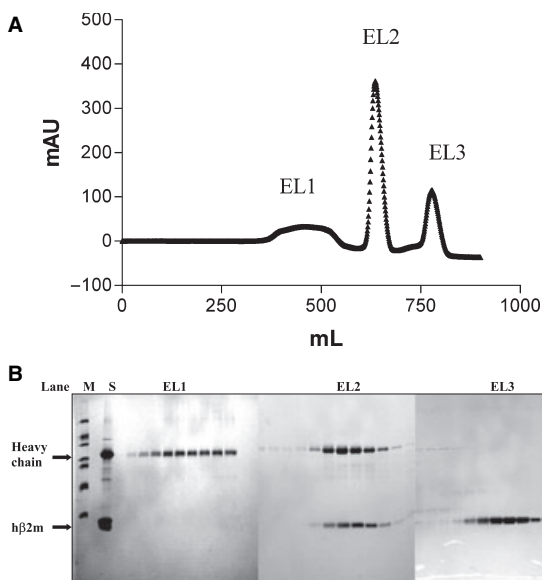


**Fig. 2.** *In vitro* refolding of shFcRn C48S/C251S. (A) Samples of *in vitro*-refolded shFcRn C48S/C251S were applied to SEC, and the complexes separated as shown in the elution profile. Fractions corresponding to three main peaks denoted EL1, EL2 and EL3 are shown. (B) Nonreducing SDS-PAGE analyses of the fractions collected (EL1, EL2 and EL3) following SEC separation. Lane M, protein marker; lane S, sample (refolding solution). The positions of HCs and of h $\beta$ 2m are indicated by black arrows.

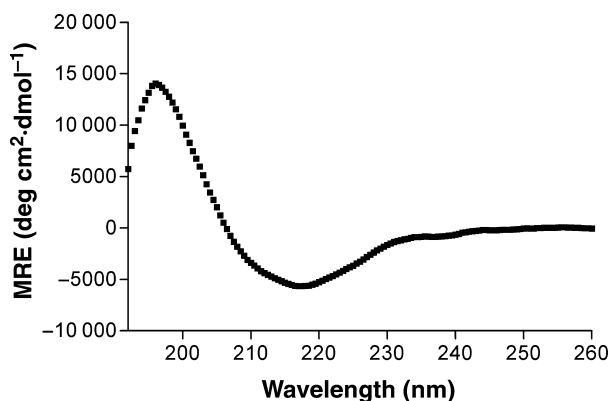


**Fig. 3.** CD structure of shFcRn C48S/C251S. Analyses of the secondary structural elements of refolded shFcRn C48S/C251S (■) were monitored by CD measurements. MRE, mean residual ellipticity.

with iodoacetamide (aliquot 1) or after sequential alkylation with iodoacetamide, reduction and alkylation by iodoacetic acid (aliquot 2). Thus, cysteine residues become alkylated by iodoacetic acid (those engaged in disulfide bonds) or iodoacetamide (free cysteines), respectively, which differ in mass by 1 Da. In the mass spectrum of h $\beta$ 2m (aliquot 1), the pronounced signal at

**Table 1.** Secondary structural elements found in shFcRn C48S/C251S.

|              | shFcRn C48S/C251S <sup>a</sup> (%) |
|--------------|------------------------------------|
| Helix        | 14.5                               |
| Antiparallel | 40.6                               |
| Parallel     | 5.4                                |
| Beta turn    | 14.7                               |
| Random coil  | 24.8                               |
| Total        | 100.0                              |

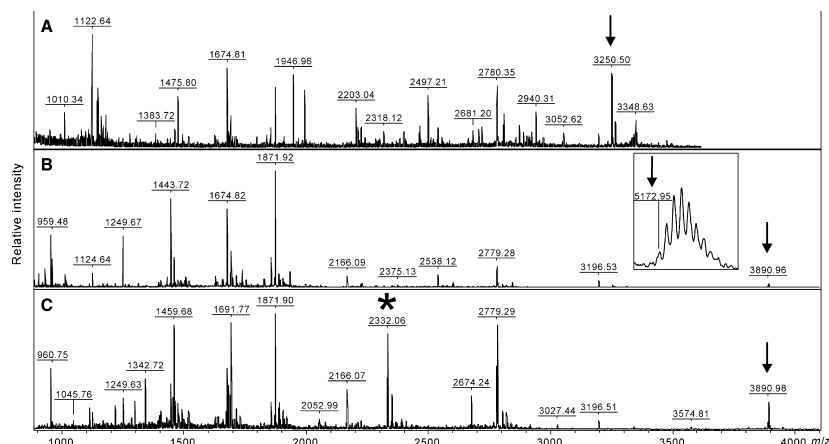
<sup>a</sup>The secondary structure elements were estimated as described previously [33] from the CD data obtained from the spectrum presented in Fig. 3.

$m/z$  3250.50 (Fig. 4A) corresponded to the two tryptic peptides containing C25 and C80 linked by a disulfide bond. Signals for these peptides alkylated by iodoacetamide were not detected, indicating a rather quantitative disulfide bond formation. Similarly, in aliquot 1 derived from hFcRn HCs, the expected disulfide bond in the  $\alpha$ 2 domain (C96–C159) was demonstrated ( $m/z$  3890.95; Fig. 4B,C). The disulfide bond in the  $\alpha$ 3 domain (C198–C252) was observed as a small signal for the mutant HC ( $m/z$  5172.95; inset in Fig. 4B), but not for the WT protein.

In aliquot 2, all four cysteine residues were found to be modified by iodoacetic acid in the mutant HC ( $m/z$  2489.22, C96;  $m/z$  1520.76, C159;  $m/z$  2915.44, C198;  $m/z$  2376.11, C252; Fig. 5A–D). In addition, for C96 and C159, smaller signals corresponding to alkylation by iodoacetamide ( $m/z$  2488.25 and 1519.77, respectively) were observed (Fig. 5A,B), indicating that disulfide formation in the  $\alpha$ 2 domain is not fully complete. The formation of the disulfide bond between C198 and C252, however, appeared to be complete (Fig. 5C,D). A similar result was obtained for C96, C159 and C198 in the hFcRn WT HC (Fig. 5E–G).

Surprisingly, residues C251 and C252 were both found to be modified by iodoacetic acid ( $m/z$  2450.09; Fig. 5H), although C251 is expected to be unpaired. The pronounced signal at  $m/z$  2332.06, marked by an asterisk in Fig. 4C (aliquot 1 of WT HC), matches the corresponding tryptic peptide assuming a disulfide bond between the vicinal residues C251 and C252. Indeed, the sequence of that peptide with an intramolecular disulfide bond was proven on a MALDI-TOF/TOF mass spectrometer (Fig. 6). Also, C48 in the  $\alpha$ 1 domain, which does not participate in disulfide bonding in a correctly folded molecule, was found to be modified by iodoacetic acid ( $m/z$  2612.13, Fig. 5I). In general, disulfide bond formation in the WT HC was far more heterogeneous, and deviations from the correct configuration were detected compared with the HC mutant.

**Fig. 4.** Analysis of  $\beta 2m$  and hFcRn HCs by MALDI-TOF MS prior to reduction of disulfide bonds (aliquot 1). Spectra were recorded after iodoacetamide treatment and tryptic digestion of gel-separated  $\beta 2m$  (A), mutant HC (B) and WT HC (C). Signals representing the expected tryptic peptides linked by a disulfide bond are indicated by an arrow. The signal at  $m/z$  in (B) is of low intensity and is given as an inset. The signal derived from the tryptic peptide with a disulfide bond between vicinal C251 and C252 is indicated by an asterisk.



### Functional properties of bacterially produced shFcRn C48S/C251S

The ligand-binding properties of refolded shFcRn C48S/C251S were assessed using SPR. Functional binding to hIgG1 was measured by injecting  $1 \mu\text{M}$  shFcRn mutant over a CM5 chip containing immobilized hIgG1 (Fig. 7A). The sensorgram demonstrates reversible, pH-dependent binding at pH 6.0 and no binding at pH 7.4. Furthermore, the equilibrium constant ( $K_D$ ) was calculated from the resonance profiles for near-equilibrium or equilibrium binding levels using BIAevaluation software after injection of 0.012–4  $\mu\text{M}$  shFcRn mutant at pH 6.0. The  $K_D$  obtained ( $1.35 \pm 0.35 \times 10^{-6} \text{ M}$ ) agrees well with that determined by others for the WT [37,38]. Mutant shFcRn was then immobilized on the chip, serial dilutions of hIgG1 or HSA were injected at pH 6.0 (Fig. 7B,C) and affinities were derived using the BIAevaluation software. Both ligands showed the expected pH-dependent binding profiles. The binding of HSA fitted well to the 1 : 1 Langmuir binding model to yield a  $K_D$  of  $1.1 \pm 0.0 \times 10^{-6} \text{ M}$ , which is in agreement with other reports [19,39]. Injection of hIgG1 over immobilized shFcRn is known to give rise to complex kinetics, and thus two relevant models were explored – the heterogeneous ligand-binding model and the bivalent analyte model – both supplemented with the BIAevaluation Wizard. The heterogeneous ligand-binding model assumes that two parallel and independent interactions ( $K_{D1}$  and  $K_{D2}$ ) take place between the ligand and the receptor, and the derived affinities were determined to be  $6.7 \pm 0.1 \times 10^{-9} \text{ M}$  ( $K_{D1}$ ) and  $219.0 \pm 37.7 \times 10^{-9} \text{ M}$  ( $K_{D2}$ ). Thus, the affinity was dramatically increased to the nM range when using this model, as has been reported previously [5,11,33]. The bivalent analyte model assumes that both sides of the symmetric Fc part of hIgG1 can interact with immobilized

shFcRn. By fitting the binding data to this model, the derived binding kinetic rates for binding to the first ligand (one side of the Fc with immobilized shFcRn) is described by a single set of rate constants,  $k_{on}$  [ $1.8 \times 10^5 \text{ (M}^{-2}\text{s}^{-1})$ ] and  $k_{off}$  [ $3.4 \times 10^{-2} \text{ s}^{-1}$ ] that yields a  $K_D$  of  $0.2 \pm 0.04 \times 10^{-6} \text{ M}$ , whereas the cooperative binding step by the second Fc side is described by a second set of rate constants,  $k_{on2}$  [ $4.4 \times 10^{-4} \text{ RU}^{-1}\text{s}^{-1}$ ] and  $k_{off2}$  [ $1.9 \times 10^{-3} \text{ s}^{-1}$ ].

Additive binding was obtained when both ligands (hIgG1 and HSA) were injected over the immobilized shFcRn mutant at pH 6.0 (Fig. 7D). Affinity measurements were also performed using a preparation of the shFcRn mutant where the N-terminal hexa-histidine tag (HAT-tag) was removed, and the resulting data exclude the possibility that the tag contributes to ligand binding (data not shown). Importantly, hFcRn binds human, rabbit and guinea-pig IgG, but it does not bind to mouse, rat, bovine or sheep IgG, with the exception of weak binding to murine IgG2b [38,40]. Samples of the 0.25  $\mu\text{M}$  shFcRn mutant were injected over high levels ( $\sim 700$ – $1000 \text{ RU}$ ) of immobilized murine IgG1 and IgG2b, with identical specificity at pH 6.0. The SPR sensorgrams showed no binding to murine IgG1 and weak binding to murine IgG2b (supplementary Fig. S4). Thus, the mutant, like the WT, discriminates between murine IgGs, and behaves like the WT also in all other aspects analyzed.

We then measured the binding of a carcinoembryonic antigen scFv–Fc antibody variant to the mutant shFcRn. This scFv–Fc, denoted H310A/H435Q, has shown promising results in preclinical tumor-imaging evaluations [24]. SPR analyses were performed using an immobilized receptor and injection of 0.5  $\mu\text{M}$  WT scFv–Fc at pH 6.0. The sensorgrams clearly demonstrate that the WT scFv–Fc interacts with shFcRn, whereas the H310A/H435Q variant does not (Fig. 7E). This explains the dramatically decreased half-life of

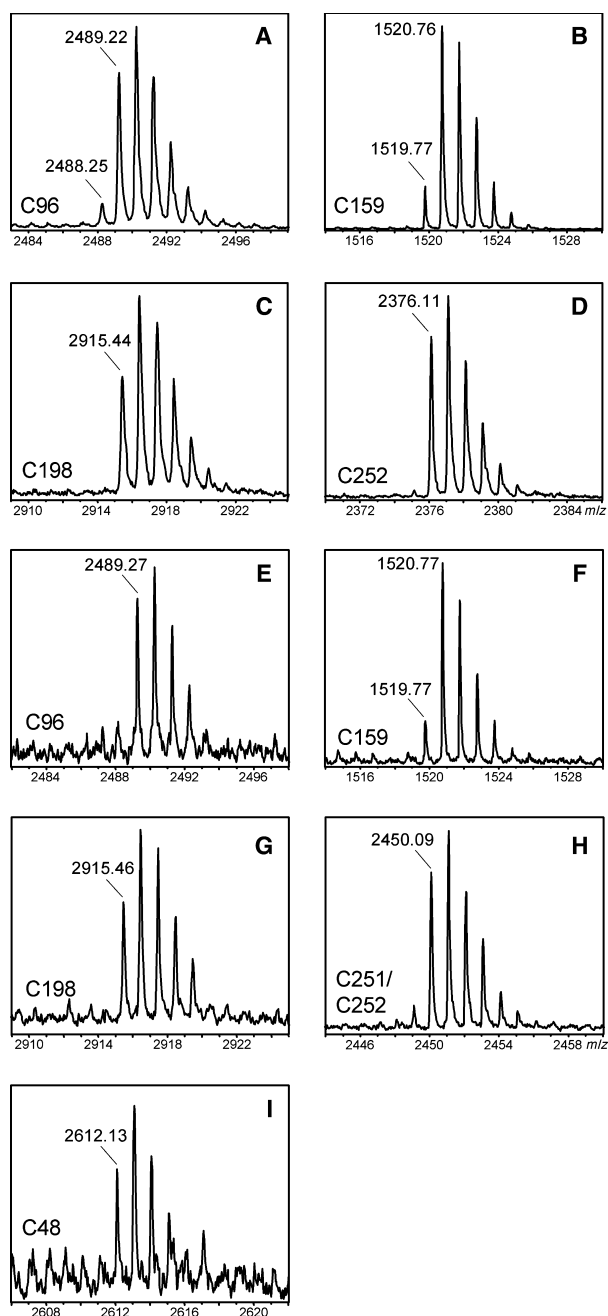


**Fig. 5.** Analysis of  $\beta$ 2m and hFcRn HCs by MALDI-TOF MS after reduction of disulfide bonds (aliquot 2). Gel-separated proteins were treated with iodoacetamide, dithiothreitol and iodoacetic acid before digestion with trypsin. Signals were derived from mutant (A–D) and WT (E–I) HC and represent tryptic peptides carrying alkylated cysteine residues. The alkylation status of the following cysteine residues was investigated: C96 (A, E), C159 (B, F), C198 (C, G), C251 (D), C251/C252 (H) and C48 (I).

H310A/H435Q compared with the WT in the anti-carcinoembryonic antigen tumor-imaging study performed in mice [24,25].

### Antigenic properties of bacterially produced FcRn C48S/C251S HC

To investigate the antigenic properties of the bacterially produced preparations, female goats were immunized with shFcRn C48S/C251S or HC. Serum collected post immunization was tested for the presence of anti-FcRn Ig in an ELISA on wells directly coated with mutant shFcRn or h $\beta$ 2m (Fig. 8A,B). While serum obtained from goat immunized with mutant shFcRn reacted towards both shFcRn and h $\beta$ 2m, serum obtained from goat immunized with HC showed no reactivity towards h $\beta$ 2m, but did bind shFcRn.

Antibodies from goat immunized with HC were purified on HC-coupled Sepharose. Elution was performed sequentially using four different buffer conditions (EL1–EL4), as described in the Materials and methods. The eluted fractions migrated as bands corresponding to 150 kDa on nonreducing SDS-PAGE and reacted in a concentration-dependent manner with mutant shFcRn in an ELISA (supplementary Fig. S5A,B). Thus, HC Sepharose affinity matrix can be utilized to purify anti-FcRn-specific Ig and, consequently, elution conditions can be chosen as desired.

Next, sera from goats immunized with the shFcRn mutant were purified in a large-scale operation on HC-coupled Sepharose. The eluted purified fractions (Fig. 8C) bound shFcRn in ELISA (Fig. 8D), while only a trace of h $\beta$ 2m reactivity was detected (Fig. 8E). Thus, the HC-coupled affinity matrix could exclude all anti-h $\beta$ 2m reactivity present in the sera.

Importantly, the purified antibody preparation from the HC-immunized goat inhibited pH-dependent binding of both ligands, IgG and HSA (Fig. 9A,B). Similar results were obtained for anti-FcRn Ig obtained from goat immunized with the shFcRn mutant (data not shown). Goat IgG from pre-immune serum purified on a protein-G column did not block the binding sites. In conclusion, these data imply that the HC, without prior assembly with h $\beta$ 2m, is sufficient for immunization to obtain binders to both ligand-binding sites on shFcRn, and that such binders may be isolated on an HC-coupled affinity matrix.

### Discussion

We have recently reported a bacterial expression strategy that generates functional nonglycosylated shFcRn WT with native binding characteristics [33]. This strategy relies on solubilization of extracted HCs in 8 M urea buffer under nonreducing conditions, a process that disrupts the tertiary structure but keeps the preformed disulfide bond configuration intact before

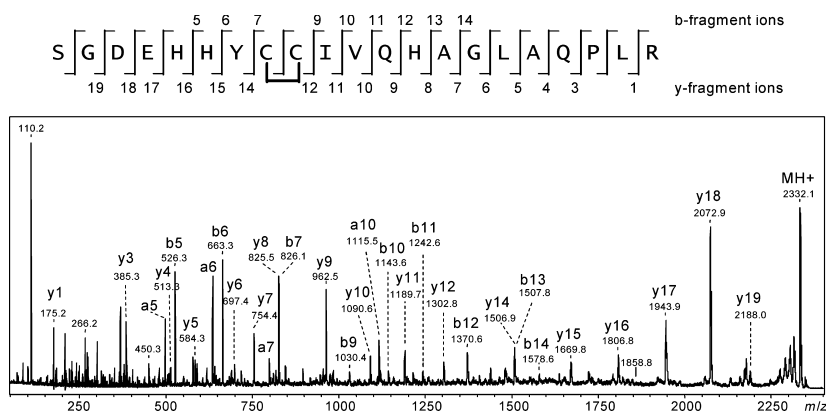


**Fig. 6.** MS/MS analysis of the tryptic peptide hFcRn WT HC 244-264 to verify the disulfide bond between vicinal cysteines 251 and 252. The ion at  $m/z$  2332.06 (Fig. 4C) was selected for fragmentation, and observed  $y$ -,  $b$ - and  $a$ -fragment ions are indicated. For an easier illustration observed  $y$ - and  $b$ -fragment ions are assigned to the sequence of peptide 244–264.

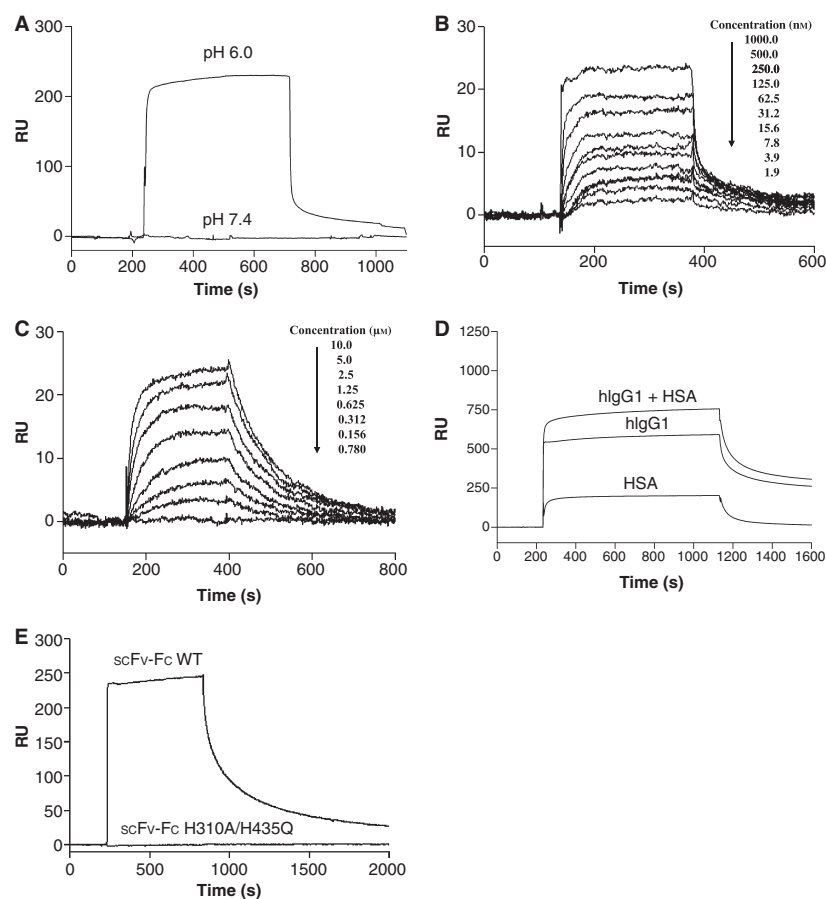


**Fig. 7.** SPR analyses of ligand binding to shFcRn C48S/C251S. (A) Binding of  $1 \mu\text{M}$  shFcRn C48S/C251S to immobilized hlgG1 at pH 6.0 and pH 7.4. (B) Concentration-dependent binding of hlgG1 to immobilized shFcRn C48S/C251S ( $\sim 100$  RU) at pH 6.0. (C) Concentration-dependent binding of HSA to immobilized shFcRn C48S/C251S ( $\sim 200$  RU) at pH 6.0. (D) The sensorgram shows a binding assay performed at pH 6.0, where  $0.5 \mu\text{M}$  hlgG1,  $30 \mu\text{M}$  HSA, or both were injected over immobilized shFcRn C48S/C251S ( $\sim 1000$ ). (E) Binding of  $0.5 \mu\text{M}$  scFv-Fc WT and scFv-Fc H310A/H435Q to immobilized shFcRn C48S/C251S at pH 6.0.

*in vitro* refolding on h $\beta$ 2m. Although the strategy was successful, only 5% of purified HCs assembled with h $\beta$ 2m.

Bacteria lack the complex folding machinery of eukaryotes, therefore, both native and scrambled disulfide bonds are formed. Furthermore, disulfide bonds may be generated in inclusion bodies and during extraction and/or purification. The situation becomes

even more complex when the protein consists of more than one subunit, such as heterodimeric FcRn.

Sequence and crystallographic analyses have shown the presence of disulfide bonds and, in addition, two unpaired cysteine residues (C48 and C251) localized to the ectodomains of the hFcRn HC [4,5]. Theoretically, 64 possible disulfide bonds can be made by the six cysteines involved. The C48S/C251S double mutant

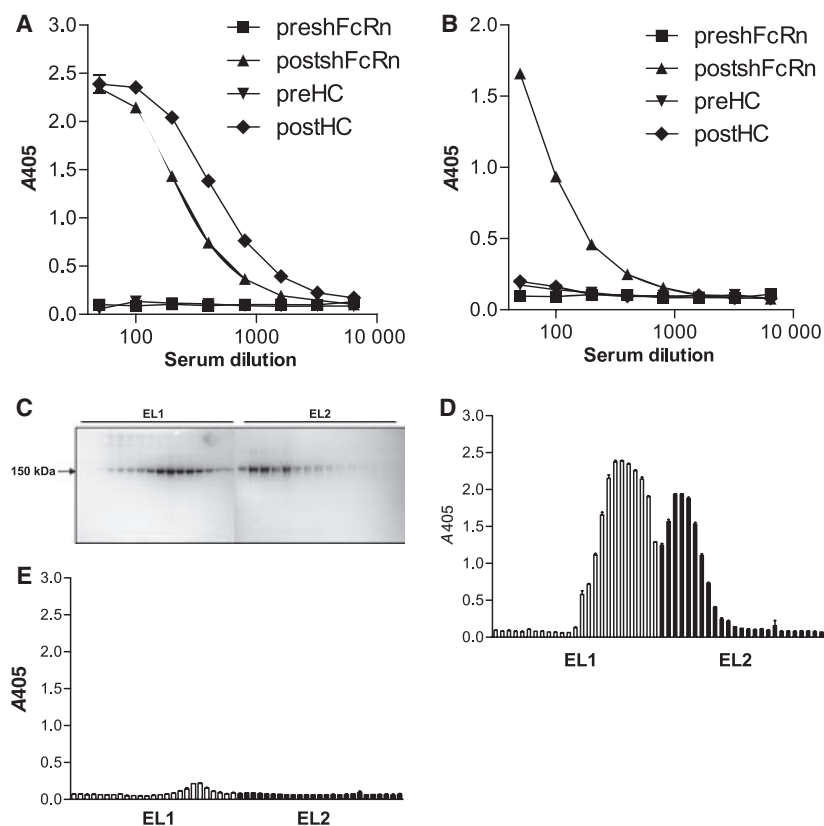


**Fig. 8.** Immunization, purification and evaluation of anti-FcRn antibody preparations. Goat sera obtained pre-immunization and post immunization with heterodimeric shFcRn mutant (preshFcRn and postshFcRn) or the mutant HC (pre-HC and post-HC) were tested in ELISA for reactivity towards (A) mutant shFcRn and (B) h $\beta$ 2m. (C) Goat antibodies obtained postimmunization with heterodimeric mutant shFcRn. Two-step elution of fractions after large-scale purification of anti-FcRn Ig and analyses by nonreducing SDS-PAGE. ELISA analyses of reactivity towards (D) mutant shFcRn and (E) h $\beta$ 2m for the corresponding fractions. The ELISA values represent the mean of triplicates. Similar data were obtained in independent experiments.

with four cysteine residues may fold into 10 possible configurations, namely one completely reduced, six partially oxidized (with one disulfide bond), and three completely oxidized (with two disulfide bonds). Initially, analyses of the double mutant expressed in a eukaryotic system using human embryonic kidney (HEK) 293E cells showed that the mutations had no effect on the production yield and pH-dependent binding to IgG. Subsequently, when the double mutant was produced in the bacterial system, we found a great effect on the refolding output. First, the amount of higher aggregates during all purification steps was dramatically decreased compared with the WT and, second, the refolded yield was 135 mg per 2 L fermentation, corresponding to an increase of  $\sim 10$ -fold compared with the WT. Even more favorably, 26% of the mutant HC assembled with h $\beta$ 2m compared with only 5% for the WT HC.

Mutant shFcRn and WT showed similar secondary structures, according to CD measurements, as described previously for WT [4,5,35,36]. Therefore, to investigate the folding of both h $\beta$ 2m and the hFcRn HCs, the configuration of disulfide bonds was qualitatively investigated using a combination of MALDI-TOF MS and chemical alkylation of cysteine residues. The expected disulfide bonds were demonstrated in

h $\beta$ 2m and the mutant. However, in the WT molecule the disulfides appeared to be more heterogeneous, with some deviations from the correct configuration. As the signal intensities for disulfide-bonded peptides tend to be low, rare disulfide-bonded peptides with incorrect oxidation may be overlooked. Tryptic peptides that carry alkylated cysteine residues are easier to detect, but then information regarding which cysteines actually pair with each other is lost. By combining the methods, a disulfide bond between vicinal cysteine residues 251 and 252 were observed in the native molecule. The influence of such a bond on the structure of the protein is difficult to predict, but disulfide bonds between adjacent cysteine residues have previously been reported to induce the formation of a tight turn (type VIII turn) of the protein backbone [41].

Replacement of the two unpaired cysteine residues with serines did not affect the functional activity of mutant shFcRn, as shown by characteristic pH-dependent binding to both ligands. In addition, no binding to murine IgG1, and only weak binding to murine IgG2b at pH 6.0, was observed, and this stringency binding is characteristic for the human receptor [38,40]. Taken together, neither C48 nor C251 are directly or indirectly involved in the stringent pH-dependent ligand binding of the soluble receptor. However, they may well be



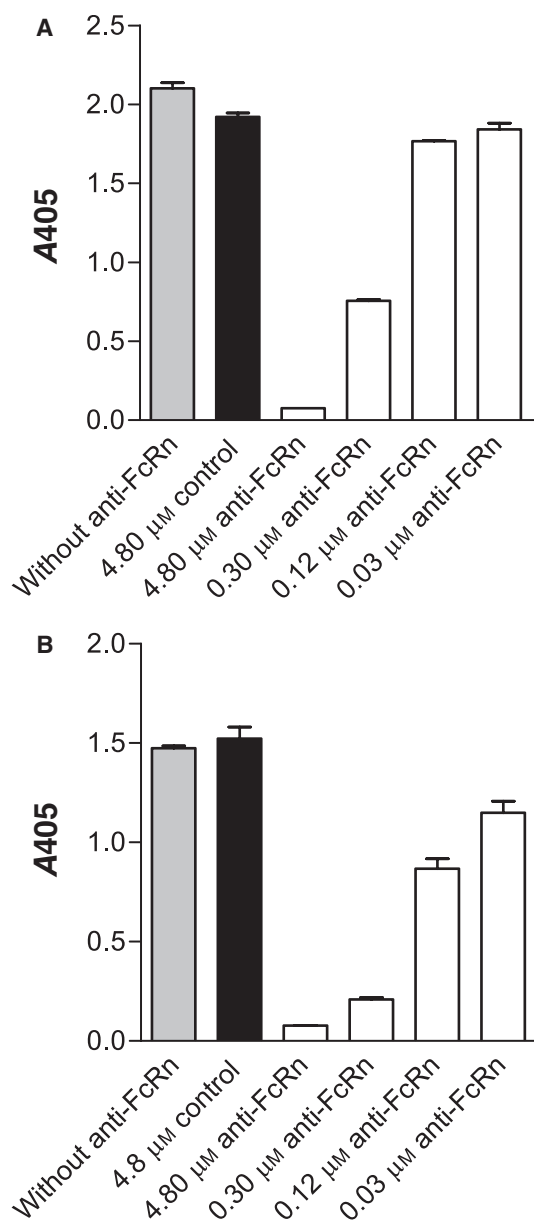


**Fig. 9.** FcRn ligand-blocking properties of anti-FcRn Ig. Serial dilutions (0.03–4.8  $\mu\text{M}$ ) of goat anti-FcRn Ig, or of proteinG-purified goat IgG from pre-immune serum, were pre-incubated with 2  $\mu\text{g}\cdot\text{mL}^{-1}$  of shFcRn–GST produced from HEK 293E cells and then tested for pH-dependent binding to (A) hIgG1 and (B) HSA at pH 6.0. The ELISA values represent the mean of triplicates. Similar data were obtained in independent experiments.

functionally important *in vivo*. Others have indicated that the membrane-anchored form of hFcRn can exist both as a noncovalent and a covalent dimer, in contrast to the secreted recombinant form of hFcRn that does not dimerize [42]. The covalent dimers are proposed to be created by interchain disulfide bonds by the exposed and available C48 and C251.

Importantly, the strategy described may prove successful for the production of other nonclassical MHC class I-related molecules as well as FcRn from different species. All HCs contain at least two intact disulfide bonds and various numbers of unpaired cysteine residues. For instance, C48 and C251 are partially conserved in published FcRn HC sequences, and several other MHC class I-related molecules contain putative unpaired cysteine residues (supplementary Tables S3 and S4).

A number of reports exists that describe the design and selection of mutant IgG molecules with altered binding to FcRn [2,20–22,30,43,44]. These involve changes of amino acids in the Fc region, either directly at the FcRn-binding interface or surrounding residues. Furthermore, any protein might be given an increased half-life by fusion to a normal or modified Fc region, as well as to albumin or to an albumin-binding molecule. One would also expect that new molecules will be selected that mimic the ability of albumin or the Fc region to bind FcRn. Several binding scaffolds with various binding specificities currently in preclinical and clinical trials may be used for such selection [45–48].

Successful selection depends on whether or not quantities of pure target are available. In this report we describe a simple and cost-effective way to generate large quantities of functional mutant shFcRn, as well as monomeric mutant HC. The antigenic properties of mutant shFcRn and the corresponding HC were investigated by immunization of goats. Goat was chosen as host because shFcRn, as well as other Fc gamma receptors, do not bind detectably to goat/sheep IgGs [40,49]. HC-coupled Sepharose affinity matrix was generated and shown to capture anti-hFcRn specific Ig from goat sera following immunization with mutant HC and shFcRn. Commonly used techniques for purification of antibodies take advantage of such affinity molecules as protein G, A and L that are directed against conserved structures, but do not distinguish between antibodies with different specificities or discriminate against irrelevant antibodies present in animal sera. Affinity purification with the mutant HC column allows purification of anti-hFcRn specific Ig. Importantly, anti-h $\beta$ 2m specific Ig are not copurified. This is important, as h $\beta$ 2m is found on all cells as part of MHC class I, in addition in other related molecules (listed in the supplementary Tables S3 and S4). We found that antibodies from immune sera bound shFcRn in ELISA when the shFcRn protein was coated in wells. One may argue that the shFcRn preparation denatures during the coating procedure, and that the serum contains antibodies that bind denatured

shFcRn. Even if such specificities are present, there is also a fraction that binds shFcRn in the native conformation. This was demonstrated in the experiment where shFcRn was pre-incubated with antibodies induced by the HC and purified on HC–Sepharose. After incubation, the shFcRn–goat antibody complexes no longer bound either of the two ligands, HSA and hIgG1. The finding that affinity-purified antibody could block pH-dependent binding of IgG and albumin to shFcRn, implies that antibodies were generated that recognized either of the ligand-binding sites located in the  $\alpha 2$  domain. Thus, the antigenic properties of the HC in this region are sufficiently similar to those found in the heterodimeric soluble receptor for HC to be utilized for immunization, purification and selection of antibodies or other binders. The HC preparation used for immunization was the same that was utilized for refolding, where 26% of the molecules were captured by h $\beta 2m$  and later found to have native disulfide bridges. Taken together, this suggests to us that the HC preparation described here may well be utilized for immunization of other mammals. The data support the idea that shFcRn as well as the mutant HC, without prior assembly with  $\beta 2m$ , is sufficient to obtain binders to either binding site on FcRn. This finding will greatly facilitate the selection and characterization of new FcRn targeting binders.

## Materials and methods

### Production and purification of eukaryotic shFcRn molecules

The cDNAs encoding truncated WT HC (amino acids 1–268) and h $\beta 2m$  (amino acids 1–99) were cloned as described previously [34]. Primers (supplementary Table S1) introduced the C48S and C251S mutations into the HC, resulting in HC C48S/C251S cDNA. The cDNA segments were subcloned in-frame of GST into pcDNA3–GST–oriP [denoted pcDNA3(oriP)–hFcRn(WT)– $\beta 2m$  and pcDNA3(oriP)–hFcRn(C48S/C251S)– $\beta 2m$ ], as described previously [34]. The constructs were transiently transfected into adherent HEK 293E cells and the supernatants were harvested [34]. Expressed shFcRn–GST fusion molecules were purified using the GSTrap™ FF 5 mL column (GE Healthcare, Oslo, Norway).

### Cloning and prokaryotic expression of hFcRn HC variants

The cDNA encoding mutant HC, without the leader sequence (amino acids 1–268), was PCR amplified as described for WT HC [33], and subsequently cloned into

pET28+ (Novagen, Darmstadt, Germany) containing a HAT-tag, denoted pET28–HAT–hFcRn (HC C48S/C251S). Plasmids were transformed into *E. coli* BL21 (DE3), as described by Stratagene. Recombinant h $\beta 2m$  cDNA was introduced and expressed in the pET28 system, as previously described [31,32]. The HAT-tag was cleaved using the Factor Xa kit from Novagen.

Expression and extraction of mutant HCs from inclusion bodies and all purification steps were performed as described previously [31,33]. SDS-PAGE analysis and refolding of purified HCs variants, in 8 M urea buffer with a fourfold molar excess of h $\beta 2m$ , were performed as described for the WT [33]. For experiments using reducing agent, 11- $\mu$ L samples of hFcRn HCs, WT and C48S/C251S (3 mg·mL<sup>-1</sup>), in 8 M urea were reduced by adding 1  $\mu$ L of 1 M  $\beta$ -mercaptoethanol (Sigma-Aldrich, Oslo, Norway). Subsequently, HCs were diluted into a 447- $\mu$ L mixture of a fourfold molar excess of h $\beta 2m$  in 50 mM Tris/glycine (pH 8.5) supplemented with 5 mM reduced glutathione (Sigma-Aldrich) and 0.5 mM oxidized glutathione (Sigma-Aldrich). The same procedure was performed in the absence of  $\beta$ -mercaptoethanol and the reduced/oxidized glutathione cocktail (Sigma-Aldrich). All samples were incubated for 1 h at room temperature (20–22°C) followed by 72 h at 4 °C before centrifugation at 20 000  $\times g$  for 15 min.

### Binding of shFcRn WT and mutant shFcRn to IgG

Binding of the shFcRn–GST variants to ligand was performed by ELISA, as previously described [19]. Human IgG coupled to Sepharose™ 6 Fast Flow or nonconjugated Sepharose (GE Healthcare) was washed in NaCl/P<sub>i</sub>, blocked in 2% skimmed milk (SM; Acumedia) then washed in NaCl/P<sub>i</sub>/0.05% Tween 20, pH 6.0 or pH 8.0. Samples of 1–5  $\mu$ g of shFcRn were diluted in 1 mL of 2% SM in NaCl/P<sub>i</sub>/0.05% Tween 20 (pH 6.0 or pH 7.4), incubated by rotation for 1 h, followed by three washing steps in 1 mL of NaCl/P<sub>i</sub>/0.05% Tween 20 at pH 6.0 or pH 7.4 on rotation for 5 min followed by centrifugation at 12 000  $g$  for 5 min between each step. After the last washing step, 100  $\mu$ L of NaCl/P<sub>i</sub>/0.05% Tween 20 at pH 7.4 was added and incubated for 1 hr on rotation followed by centrifugation at 12 000  $g$ . The pooled fractions were separated by SDS-PAGE (12% gel) (Bio-Rad Laboratories, Hercules, CA, USA) and then blotted onto a poly(vinylidene fluoride) membrane (Millipore Corporation, Bedford, MA, USA) in Tris/glycine buffer at 100 V for 1.5 h. The membranes were blocked in NaCl/P<sub>i</sub> containing 4% SM for 1 h at room temperature (20–22°C), washed in NaCl/P<sub>i</sub>/0.05% Tween 20 and incubated with goat anti-hFcRn (G3290) serum followed by mouse anti-goat horseradish peroxidase (Sigma-Aldrich) at room temperature (20–22°C) for 1 h. Then, the membranes were washed thoroughly with NaCl/P<sub>i</sub>/0.05% Tween 20, incubated in a mixture of

SuperSignal solution (Pierce Chemical Co., Rockford, IL) for 1 min, after which the reactions were visualized on a Kodak XAR film.

## CD

CD spectra were recorded, and secondary-structure elements and thermal stability were estimated, as previously described [33].

## Production of goat antisera

Female goats were immunized subcutaneously with 50  $\mu\text{g}$  of mutant shFcRn or mutant HC in 500  $\mu\text{L}$  of NaCl/P<sub>i</sub> (pH 7.3) and 750  $\mu\text{L}$  of Freund's complete adjuvant (Difco, Detroit, MI, USA). On day 11 a booster dose (50  $\mu\text{g}$ ) was given with Freund's incomplete adjuvant (Difco), and repeated after 24, 66 and 105 days, and the collected and pooled sera were denoted G3290 (mutant shFcRn) and G2248 (mutant HC). The experiments were conducted in accordance with the laws and regulations controlling procedures in live animals in Norway (Norwegian Institute of Public Health).

## Binding studies using SPR

Biacore 3000 (GE Healthcare) was used and CM5 sensor chips were coupled with hIgG1 (~1200 RU), mouse IgG1 (~1000 RU), mouse IgG2b (~700 RU) or shFcRn C48/C251S (100–1000 RU) using amine coupling chemistry, all as described by the manufacturer. The coupling was performed by injecting 10–12  $\mu\text{g}\cdot\text{mL}^{-1}$  of each protein into 10 mM sodium acetate, pH 5.0 (GE Healthcare). All experiments were performed in phosphate buffer (67 mM phosphate buffer, 0.15 M NaCl) at pH 6.0 or pH 7.4, or in HBS/EP buffer (0.01 M HEPES, 0.15 M NaCl, 3 mM EDTA, 0.005% Surfactant P20) at pH 7.4 (GE Healthcare).

Dilutions (4–0.012  $\mu\text{M}$ ) of mutant shFcRn were injected over immobilized hIgG1 or HSA, or dilutions of HSA (10–0.7  $\mu\text{M}$ ), hIgG1 (1–0.003  $\mu\text{M}$ ), scFv–Fc WT (0.5  $\mu\text{M}$ ) and scFv–Fc H310A/H435Q (0.5  $\mu\text{M}$ ) were injected over immobilized mutant shFcRn. Samples of 0.25  $\mu\text{M}$  shFcRn mutant was injected over mouse IgG1 and mouse IgG2b. The scFv–Fc WT and H310A/H435Q variants were produced as previously described [24]. All experiments were performed at a flow rate of 30–50  $\mu\text{L}\cdot\text{min}^{-1}$  at 25 °C.

The flow cells were 'stripped' after each dissociation phase over immobilized shFcRn mutant in phosphate buffer at pH 7.4. In competitive analyses, 30  $\mu\text{M}$  HSA and 0.5  $\mu\text{M}$  hIgG1 were injected alone or together at pH 6.0 over immobilized shFcRn mutant. In all experiments, data were zero adjusted and the reference cell value subtracted. Binding analyses were performed using

the Langmuir binding model (1 : 1 binding interaction), the heterogeneous ligand-binding model or the bivalent analyte binding model supplemented with the BIAevaluation wizard.

## ELISA analyses of anti-FcRn reactivity

Wells of ELISA plates were coated with 100  $\mu\text{L}$  of mutant shFcRn or h $\beta$ 2m (Abcam) at 2  $\mu\text{g}\cdot\text{mL}^{-1}$ , and blocked with 4% SM (Acumedia) for 1 h. Collected sera taken pre-immunization and postimmunization (G3290 and G2248) were diluted, added to the wells and incubated for 1 h at 20–22 °C. Bound anti-FcRn Ig was detected using horseradish peroxidase-conjugated protein G (Calbiochem, Darmstadt, Germany). The ELISAs were developed by adding 100  $\mu\text{L}$  of substrate 2,2'-azinobis(3-ethylbenzo-6-thiazoline-sulfonic acid)/H<sub>2</sub>O<sub>2</sub> (Sigma-Aldrich).

## Preparation of a HC column

Small-scale and large-scale coupling were performed using urea-dissolved mutant HC at 0.001–0.64  $\text{mg}\cdot\text{mL}^{-1}$  and N-hydroxysuccinimide-activated Sepharose 4 Fast Flow matrix (GE Healthcare), as recommended by the manufacturer. Sera were applied to the mutant HC-coupled matrix equilibrated with 1 $\times$  NaCl/P<sub>i</sub>, followed by 5–10 column volumes of washing with a flow rate of 3–5  $\text{mL}\cdot\text{min}^{-1}$ . Bound antibodies were sequentially eluted with an unchanged flow rate using 0.1 M glycine/HCl, pH 2.2, 0.1 M glycine/HCl, pH 1.5, 2.0 M guanidine/HCl, pH 5.0 and 4.0 M guanidine/HCl, pH 5.0 (small scale), or 20–25 mL of 0.1 M glycine/HCl, pH 2.2, followed by 4 M guanidine/HCl, pH 5.0 (large scale). Fractions were eluted into 1 M Tris/HCl (pH 9.0) and subjected to 12% nonreducing SDS-PAGE (Bio-Rad Laboratories) analyses. Fractions were pooled, the buffer was changed and the samples were concentrated using Amicon Plus 20 (YM-50) centrifugal filter devices (Millipore) and stored at 4 °C. Total goat IgG was purified from sera samples using a commercial protein G-coupled affinity matrix (GE Healthcare).

## Inhibition of IgG and HSA binding by anti-FcRn

Inhibition of IgG and HSA binding was performed using pH-dependent ELISA assays, as described previously [19], except that 100  $\mu\text{L}$  of anti-5-iodo-4-hydroxy-3-nitro-phenacetyl (NIP) hIgG1 (0.5  $\mu\text{g}\cdot\text{mL}^{-1}$ ) was added to each well and incubated for 1 h at 20–22 °C. Then the wells were washed four times with NaCl/P<sub>i</sub>/0.05% Tween 20, pH 6.0. shFcRn–GST (2  $\text{mg}\cdot\text{mL}^{-1}$ ) was pre-incubated with purified anti-hFcRn HC goat Ig (0.03–4.8  $\mu\text{M}$ ) or pre-immune goat IgG (4.8  $\mu\text{M}$ ), in NaCl/P<sub>i</sub>/0.05% Tween 20, pH 6.0, for 30 min at room temperature (20–22 °C), and then 100  $\mu\text{L}$  was added to each well.

## Acknowledgements

This work was supported by grants from the Steering board for Research in Molecular Biology, Biotechnology and Bioinformatics (EMBIO) at the University of Oslo (JTA), The Norwegian Research Council (155231) and Norwegian Cancer Society (B95078), both for IS, and EU (6FP503231) for SB. The authors wish to thank Dimitrios Mantzilas (Department of Molecular Biosciences, University of Oslo) for his assistance with the CD analysis, the Proteomics Core Facility at Rikshospitalet University Hospital for mass spectrometric analysis, Søren Andersen and Professor Peter Roepstorff (University of Southern Denmark, Odense) for recording the presented MALDI-TOF/TOF spectrum, and Tove Olafsen and Anna M. Wu (University of California Los Angeles, USA) for critical manuscript revision.

## References

- Anderson CL, Chaudhury C, Kim J, Bronson CL, Wani MA & Mohanty S (2006) Perspective – FcRn transports albumin: relevance to immunology and medicine. *Trends Immunol* **27**, 343–348.
- Roopenian DC & Akilesh S (2007) FcRn: the neonatal Fc receptor comes of age. *Nat Rev Immunol* **7**, 715–725.
- Ghetie V, Hubbard JG, Kim JK, Tsen MF, Lee Y & Ward ES (1996) Abnormally short serum half-lives of IgG in beta 2-microglobulin-deficient mice. *Eur J Immunol* **26**, 690–696.
- Burmeister WP, Huber AH & Bjorkman PJ (1994) Crystal structure of the complex of rat neonatal Fc receptor with Fc. *Nature* **372**, 379–383.
- West AP Jr & Bjorkman PJ (2000) Crystal structure and immunoglobulin G binding properties of the human major histocompatibility complex-related Fc receptor. *Biochemistry* **39**, 9698–9708.
- Halliday R (1955) Prenatal and postnatal transmission of passive immunity to young rats. *Proc R Soc Lond B Biol Sci* **144**, 427–430.
- Martin MG, Wu SV & Walsh JH (1997) Ontogenetic development and distribution of antibody transport and Fc receptor mRNA expression in rat intestine. *Dig Dis Sci* **42**, 1062–1069.
- Ellinger I, Schwab M, Stefanescu A, Hunziker W & Fuchs R (1999) IgG transport across trophoblast-derived BeWo cells: a model system to study IgG transport in the placenta. *Eur J Immunol* **29**, 733–744.
- Leach JL, Sedmak DD, Osborne JM, Rahill B, Lairmore MD & Anderson CL (1996) Isolation from human placenta of the IgG transporter, FcRn, and localization to the syncytiotrophoblast: implications for maternal-fetal antibody transport. *J Immunol* **157**, 3317–3322.
- Vaccaro C, Bawdon R, Wanjie S, Ober RJ & Ward ES (2006) Divergent activities of an engineered antibody in murine and human systems have implications for therapeutic antibodies. *Proc Natl Acad Sci USA* **103**, 18709–18714.
- Bitonti AJ, Dumont JA, Low SC, Peters RT, Kropp KE, Palombella VJ, Stattel JM, Lu Y, Tan CA, Song JJ *et al.* (2004) Pulmonary delivery of an erythropoietin Fc fusion protein in non-human primates through an immunoglobulin transport pathway. *Proc Natl Acad Sci USA* **101**, 9763–9768.
- Dickinson BL, Badizadegan K, Wu Z, Ahouse JC, Zhu X, Simister NE, Blumberg RS & Lencer WI (1999) Bidirectional FcRn-dependent IgG transport in a polarized human intestinal epithelial cell line. *J Clin Invest* **104**, 903–911.
- Spiekermann GM, Finn PW, Ward ES, Dumont J, Dickinson BL, Blumberg RS & Lencer WI (2002) Receptor-mediated immunoglobulin G transport across mucosal barriers in adult life: functional expression of FcRn in the mammalian lung. *J Exp Med* **196**, 303–310.
- Low SC, Nunes SL, Bitonti AJ & Dumont JA (2005) Oral and pulmonary delivery of FSH-Fc fusion proteins via neonatal Fc receptor-mediated transcytosis. *Hum Reprod* **20**, 1805–1813.
- Akilesh S, Christianson GJ, Roopenian DC & Shaw AS (2007) Neonatal FcR expression in bone marrow-derived cells functions to protect serum IgG from catabolism. *J Immunol* **179**, 4580–4588.
- Zhu X, Meng G, Dickinson BL, Li X, Mizoguchi E, Miao L, Wang Y, Robert C, Wu B, Smith PD *et al.* (2001) MHC class I-related neonatal Fc receptor for IgG is functionally expressed in monocytes, intestinal macrophages, and dendritic cells. *J Immunol* **166**, 3266–3276.
- Vidarsson G, Stemerding AM, Stapleton NM, Spliethoff SE, Janssen H, Rebers FE, de Haas M & van de Winkel JG (2006) FcRn: an IgG receptor on phagocytes with a novel role in phagocytosis. *Blood* **108**, 3573–3579.
- Kim JK, Tsen MF, Ghetie V & Ward ES (1994) Identifying amino acid residues that influence plasma clearance of murine IgG1 fragments by site-directed mutagenesis. *Eur J Immunol* **24**, 542–548.
- Andersen JT, Dee Qian J & Sandlie I (2006) The conserved histidine 166 residue of the human neonatal Fc receptor heavy chain is critical for the pH-dependent binding to albumin. *Eur J Immunol* **36**, 3044–3051.
- Hinton PR, Johlfs MG, Xiong JM, Hanestad K, Ong KC, Bullock C, Keller S, Tang MT, Tso JY, Vasquez M *et al.* (2004) Engineered human IgG antibodies with longer serum half-lives in primates. *J Biol Chem* **279**, 6213–6216.

- 21 Hinton PR, Xiong JM, Johlfs MG, Tang MT, Keller S & Tsurushita N (2006) An engineered human IgG1 antibody with longer serum half-life. *J Immunol* **176**, 346–356.
- 22 Petkova SB, Akilesh S, Sproule TJ, Christianson GJ, Al Khabbaz H, Brown AC, Presta LG, Meng YG & Roopenian DC (2006) Enhanced half-life of genetically engineered human IgG1 antibodies in a humanized FcRn mouse model: potential application in humorally mediated autoimmune disease. *Int Immunol* **18**, 1759–1769.
- 23 Hornick JL, Sharifi J, Khawli LA, Hu P, Bai WG, Alauddin MM, Mizokami MM & Epstein AL (2000) Single amino acid substitution in the Fc region of chimeric TNT-3 antibody accelerates clearance and improves immunoscintigraphy of solid tumors. *J Nucl Med* **41**, 355–362.
- 24 Kenanova V, Olafsen T, Crow DM, Sundaresan G, Subbarayan M, Carter NH, Ikle DN, Yazaki PJ, Chatzioannou AF, Gambhir SS *et al.* (2005) Tailoring the pharmacokinetics and positron emission tomography imaging properties of anti-carcinoembryonic antigen single-chain Fv-Fc antibody fragments. *Cancer Res* **65**, 622–631.
- 25 Kenanova V, Olafsen T, Williams LE, Ruel NH, Longmate J, Yazaki PJ, Shively JE, Colcher D, Raubitschek AA & Wu AM (2007) Radioiodinated versus radiometal-labeled anti-carcinoembryonic antigen single-chain Fv-Fc antibody fragments: optimal pharmacokinetics for therapy. *Cancer Res* **67**, 718–726.
- 26 Halpern W, Riccobene TA, Agostini H, Baker K, Stolow D, Gu ML, Hirsch J, Mahoney A, Carrell J, Boyd E *et al.* (2002) Albugranin, a recombinant human granulocyte colony stimulating factor (G-CSF) genetically fused to recombinant human albumin induces prolonged myelopoietic effects in mice and monkeys. *Pharm Res* **19**, 1720–1729.
- 27 Osborn BL, Sekut L, Corcoran M, Poortman C, Sturm B, Chen G, Mather D, Lin HL & Parry TJ (2002) Albutropin: a growth hormone-albumin fusion with improved pharmacokinetics and pharmacodynamics in rats and monkeys. *Eur J Pharmacol* **456**, 149–158.
- 28 Roopenian DC, Christianson GJ, Sproule TJ, Brown AC, Akilesh S, Jung N, Petkova S, Avanesian L, Choi EY, Shaffer DJ *et al.* (2003) The MHC class I-like IgG receptor controls perinatal IgG transport, IgG homeostasis, and fate of IgG-Fc-coupled drugs. *J Immunol* **170**, 3528–3533.
- 29 Subramanian GM, Fiscella M, Lamouse-Smith A, Zeuzem S & McHutchison JG (2007) Albinterferon alpha-2b: a genetic fusion protein for the treatment of chronic hepatitis C. *Nat Biotechnol* **25**, 1411–1419.
- 30 Vaccaro C, Zhou J, Ober RJ & Ward ES (2005) Engineering the Fc region of immunoglobulin G to modulate in vivo antibody levels. *Nat Biotechnol* **23**, 1283–1288.
- 31 Ferre H, Ruffet E, Blicher T, Sylvester-Hvid C, Nielsen LL, Hogley TJ, Thomas OR & Buus S (2003) Purification of correctly oxidized MHC class I heavy-chain molecules under denaturing conditions: a novel strategy exploiting disulfide assisted protein folding. *Protein Sci* **12**, 551–559.
- 32 Ostergaard Pedersen L, Nissen MH, Hansen NJ, Nielsen LL, Lauenmoller SL, Blicher T, Nansen A, Sylvester-Hvid C, Thromsen AR & Buus S (2001) Efficient assembly of recombinant major histocompatibility complex class I molecules with preformed disulfide bonds. *Eur J Immunol* **31**, 2986–2996.
- 33 Andersen JT, Justesen S, Berntzen G, Michaelsen TE, Lauvrak V, Fleckenstein B, Buus S & Sandlie I (2007) A strategy for bacterial production of a soluble functional human neonatal Fc receptor. *J Immunol Methods* **331**, 39–49.
- 34 Berntzen G, Lunde E, Flobakk M, Andersen JT, Lauvrak V & Sandlie I (2005) Prolonged and increased expression of soluble Fc receptors, IgG and a TCR-Ig fusion protein by transiently transfected adherent 293E cells. *J Immunol Methods* **298**, 93–104.
- 35 Burmeister WP, Gastinel LN, Simister NE, Blum ML & Bjorkman PJ (1994) Crystal structure at 2.2 Å resolution of the MHC-related neonatal Fc receptor. *Nature* **372**, 336–343.
- 36 Gastinel LN, Simister NE & Bjorkman PJ (1992) Expression and crystallization of a soluble and functional form of an Fc receptor related to class I histocompatibility molecules. *Proc Natl Acad Sci USA* **89**, 638–642.
- 37 Firan M, Bawdon R, Radu C, Ober RJ, Eaken D, Antohe F, Ghetie V & Ward ES (2001) The MHC class I-related receptor, FcRn, plays an essential role in the maternofetal transfer of gamma-globulin in humans. *Int Immunol* **13**, 993–1002.
- 38 Zhou J, Mateos F, Ober RJ & Ward ES (2005) Confering the binding properties of the mouse MHC class I-related receptor, FcRn, onto the human ortholog by sequential rounds of site-directed mutagenesis. *J Mol Biol* **345**, 1071–1081.
- 39 Chaudhury C, Brooks CL, Carter DC, Robinson JM & Anderson CL (2006) Albumin binding to FcRn: distinct from the FcRn-IgG interaction. *Biochemistry* **45**, 4983–4990.
- 40 Ober RJ, Radu CG, Ghetie V & Ward ES (2001) Differences in promiscuity for antibody-FcRn interactions across species: implications for therapeutic antibodies. *Int Immunol* **13**, 1551–1559.
- 41 Carugo O, Cemazar M, Zahariev S, Hudaky I, Gaspari Z, Perczel A & Pongor S (2003) Vicinal disulfide turns. *Protein Eng* **16**, 637–639.
- 42 Praetor A, Jones RM, Wong WL & Hunziker W (2002) Membrane-anchored human FcRn can oligomerize in the absence of IgG. *J Mol Biol* **321**, 277–284.

- 43 Dall'Acqua WF, Kiener PA & Wu H (2006) Properties of human IgG1s engineered for enhanced binding to the neonatal Fc receptor (FcRn). *J Biol Chem* **281**, 23514–23524.
- 44 Ghetie V, Popov S, Borvak J, Radu C, Matesoi D, Medesan C, Ober RJ & Ward ES (1997) Increasing the serum persistence of an IgG fragment by random mutagenesis. *Nat Biotechnol* **15**, 637–640.
- 45 Binz HK, Amstutz P & Pluckthun A (2005) Engineering novel binding proteins from nonimmunoglobulin domains. *Nat Biotechnol* **23**, 1257–1268.
- 46 Holt LJ, Herring C, Jespers LS, Woolven BP & Tomlinson IM (2003) Domain antibodies: proteins for therapy. *Trends Biotechnol* **21**, 484–490.
- 47 Revets H, De Baetselier P & Muyldermans S (2005) Nanobodies as novel agents for cancer therapy. *Expert Opin Biol Ther* **5**, 111–124.
- 48 Stumpp MT & Amstutz P (2007) DARPin: a true alternative to antibodies. *Curr Opin Drug Discov Devel* **10**, 153–159.
- 49 Alexander EL & Sanders SK (1977) F(ab')<sub>2</sub> reagents are not required if goat, rather than rabbit, antibodies are used to detect human surface immunoglobulin. *J Immunol* **119**, 1084–1088.

## Supplementary material

The following supplementary material is available online:

**Fig. S1.** pH-dependent binding of shFcRn–GST variants to hIgG-coupled Sepharose.

**Fig. S2.** Boiled and reduced samples of hFcRn C48S/C251S HC analyzed by SDS-PAGE (12% gel).

**Fig. S3.** Nonreducing SDS-PAGE analyses after classical reduction/oxidation *in vitro* refolding versus oxidative disulfide-assisted *in vitro* refolding.

**Fig. S4.** Binding of mIgG1 and mIgG2b to the shFcRn mutant.

**Fig. S5.** Nonreducing SDS-PAGE separation and ELISA of antibodies eluted sequentially from HC-coupled Sepharose 4 Fast Flow matrix.

**Table S1.** Primer sequences.

**Table S2.** Summary of purification and refolding steps for human HC variants.

**Table S3.** Numbers of cysteine residues of FcRn HCs across species<sup>a</sup>.

**Table S4.** Numbers of cysteine residues of nonclassical MHC class I HC<sup>a</sup>.

This material is available as part of the online article from <http://www.blackwell-synergy.com>

Please note: Blackwell Publishing are not responsible for the content or functionality of any supplementary materials supplied by the authors. Any queries (other than missing material) should be directed to the corresponding author for the article.